MM-PB/SA method, the water molecules were replaced with implicit solvation models. The binding free energy was calculated by the following equations.

$$\Delta G_{bind} = G_{complex} - (G_{protein} + G_{ligand}) \quad (2)$$

$$G = < E_{MM} > + < G_{PB} > + < G_{SA} > - TS \quad (3)$$

$$E_{MM} = E_{\text{int}} + E_{ele} + E_{vdW} \quad (4)$$

$$G_{SA} = \gamma A + b \quad (5)$$

In the above equations, $< >$ denotes the average for a set of 30 conformations along an MD trajectory. E_{int} includes the bond, angle, and torsional angle energies; E_{ele} and E_{vdW} represent the intermolecular electrostatic and van der Waals energies, respectively. G_{PB} was calculated by solving the PB equation with the DelPhi program [69,70], using the PARSE radii [71,72] and AMBER charges. The grid spacing used was 0.5 Å. The dielectric constants inside and outside the molecule were 1.0 and 80.0, respectively. In equation 5, which calculates the nonpolar solvation contribution, A is the solvent-accessible surface area that was calculated using the Michael Sanner's Molecular Surface (MSMS) program [73], and γ and b are 0.00542 kcal/mol-Å^2 and 0.92 kcal/mol, respectively. The probe radius was 1.4 Å. The conformational entropy term of the solute, TS, was approximated by a combination of a classical statistics expression and PCA [74], using the PTRAJ module of AMBER 8.0 [63]. In the PCA calculation, the last 210 ps (3,000 conformations) of each production trajectory were used.

The analysis of the binding free energy involved the calculation of the energies for conformations obtained from the MM (namely, energy-minimized) coordinates or MD trajectories. When the MM calculations or MD simulations of a complex, protein, and ligand were performed, we could obtain various types of binding free energies by combining the respective coordinate sets. The enthalpy contributions of G_{protein} and G_{ligand} in equation 2 were calculated in the following 2 ways: (1) by using the coordinate sets of a protein (or ligand) obtained from the MD simulations (or MM calculations) of the protein (or ligand) and (2) by using the coordinate sets extracted from the MD simulation of a complex. Similar to the enthalpy contribution, the entropy contribution was calculated by using the MD trajectories. When the entropy contributions of G_{complex}, G_{protein}, and G_{ligand} were calculated by using the MD trajectory of only the complex, we considered the entropy contribution of ΔG_{bind} to be zero because the energy components were almost cancelled. In this study, in order to thoroughly investigate which MM/PB-SA energies were suitable for compound screening, we adopted 12 binding free energies, G01–G12, to manage the entropy contributions independently of the enthalpy contributions (see Table 1). It should be noted that the coordinate sets for calculating the entropy contributions were not always consistent with those for calculating enthalpy contributions. Table 1 shows the enthalpy and entropy terms for computing of G_{complex}, G_{protein}, and G_{ligand} in equation 2. We classified the 12 binding free energies into four categories. Category 1 contained the energies obtained by the MM calculations, and categories 2, 3, and 4 contained those obtained by MD calculations. These categories were classified according to the combination of coordinate sets used for enthalpy calculations: G01–G03, G04–G06, G07–G09, and G10–G12 belonged to categories 1, 2, 3, and 4, respectively. Each binding free energy of a ligand adopts the minimum energies from among the energies of multiple poses. Thus, by gathering and arranging their energies, we were able to assess the enrichment performance of the screening approach.

Supporting Information

Figure S1 Active compounds of trypsin. The structural formulae and PDB ids of active compounds used in the seeded compound library are shown in the following figures. The asterisks represent the active compounds in top-scoring 1,000.
Found at: doi:10.1371/journal.pcbi.1000528.s001 (0.08 MB DOC)

Figure S2 Active compounds of HIV PR. The structural formulae and PDB ids of active compounds used in the seeded compound library are shown in the following figures. The asterisks represent the active compounds in top-scoring 1,000.
Found at: doi:10.1371/journal.pcbi.1000528.s002 (0.53 MB DOC)

Figure S3 Active compounds of AChE. The structural formulae and PDB ids of active compounds used in the seeded compound library are shown in the following figures. The asterisks represent the active compounds in top-scoring 1,000.
Found at: doi:10.1371/journal.pcbi.1000528.s003 (0.06 MB DOC)

Figure S4 Active compounds of CDK2. The structural formulae and PDB ids of active compounds used in the seeded compound library are shown in the following figures. The asterisks represent the active compounds in top-scoring 1,000. Compounds 1 and 19 were selected by referencing literatures.
Found at: doi:10.1371/journal.pcbi.1000528.s004 (0.11 MB DOC)

Figure S5 Number of correctly docked conformations in top-scored active compounds. These indicate the number of correctly docked conformations in the top-scoring poses for active compounds obtained from molecular docking, G01, and G06. The red and blue bars indicate the number of poses within the root mean square deviations (RMSDs) of 2.5 and 3.5 Å from those of the experimental structure, respectively. The active compounds in the top 1,000 were investigated. In G06, the final MD structure was used.
Found at: doi:10.1371/journal.pcbi.1000528.s005 (0.10 MB DOC)

Figure S6 Minimal RMSD values of computed poses from experimental poses for active compounds. The horizontal axis indicates the index number of active compounds in the top 1,000 shown in Figures S1, S2, S3, S4 and the vertical axis indicates the minimal RMSD among all the poses. For each protein, the poses obtained from molecular docking, G01, and G06 were investigated. In G06, the final MD structure was used. The red bars indicate the pose within the top-three scoring. For trypsin, HIV PR, and AChE, it was found that MD simulations could improve the binding modes and predict better binding free energies. For CDK2, however, it is suggested that MD simulations lead to structural uncertainties and an inaccurate estimation of the binding free energy.
Found at: doi:10.1371/journal.pcbi.1000528.s006 (0.24 MB DOC)

Figure S7 ROC curves using molecular weight as classifier. This graph shows the sensitivity versus 1-specificity. This indicates

ROC curves when the active compounds in the top 1,000 compounds are considered as total the true positives. ROC curves for trypsin, HIV PR, AChE, and CDK2 were drawn in blue, red, yellow, and orange, respectively. These ROC values for trypsin, HIV PR, AChE, and CDK2 are 0.454, 0.674, 0.462, and 0.430. From statistical analysis, it is obvious that the differences in the ROC values between G06 and molecular weight were statistically significant for trypsin, HIV PR, AChE. The differences in the ROC values between molecular docking and molecular weight were not statistically significant for all proteins.
Found at: doi:10.1371/journal.pcbi.1000528.s007 (0.08 MB DOC)

Text S1 Assignment of missing force field parameters. We filled in the following missing parameters on the basis of the information on regarding atom types, bonds, valences, angles, and dihedrals by using an in-house program.
Found at: doi:10.1371/journal.pcbi.1000528.s008 (0.06 MB DOC)

Author Contributions

Conceived and designed the experiments: NO AS MT. Performed the experiments: NO NF HF. Analyzed the data: NO NF. Contributed reagents/materials/analysis tools: NO NF HF GM RY YO TN. Wrote the paper: NO AS MT.

References

1. Young K, Lin S, Sun L, Lee E, Modi M, et al. (1998) Identification of a calcium channel modulator using a high throughput yeast two-hybrid screen. Nat Biotechnol 16: 946–950.
2. Hamasaki K, Rando RR (1998) A high-throughput fluorescence screen to monitor the specific binding of antagonists to RNA targets. Anal Biochem 261: 183–190.
3. Moore KJ, Turconi S, Miles-Williams A, Djaballah H, Hurskainen P, et al. (1999) A Homogenous 384-Well High Throughput Screen for Novel Tumor Necrosis Factor Receptor: Ligand Interactions Using Time Resolved Energy Transfer. J Biomol Screen 4: 205–214.
4. Dunn D, Orlowski M, McCoy P, Gastgeb F, Appell K, et al. (2000) Ultra-high throughput screen of two-million-member combinatorial compound collection in a miniaturized, 1536-well assay format. J Biomol Screen 5: 177–188.
5. Doman TN, McGovern SL, Witherbee BJ, Kasten TP, Kurumbail R, et al. (2002) Molecular docking and high-throughput screening for novel inhibitors of protein tyrosine phosphatase-1B. J Med Chem 45: 2213–2221.
6. Chen J, Zhang Z, Stebbins JL, Zhang X, Hoffman R, et al. (2007) A fragment-based approach for the discovery of isoform-specific p38alpha inhibitors. ACS Chem Biol 2: 329–336.
7. Carr RA, Congreve M, Murray CW, Rees DC (2005) Fragment-based lead discovery: leads by design. Drug Discov Today 10: 987–992.
8. Hann MM, Leach AR, Harper G (2001) Molecular complexity and its impact on the probability of finding leads for drug discovery. J Chem Inf Comput Sci 41: 856–864.
9. Jones G, Willett P, Glen RC (1995) Molecular recognition of receptor sites using a genetic algorithm with a description of desolvation. J Mol Biol 245: 43–53.
10. Jones G, Willett P, Glen RC, Leach AR, Taylor R (1997) Development and validation of a genetic algorithm for flexible docking. J Mol Biol 267: 727–748.
11. Ewing TJ, Makino S, Skillman AG, Kuntz ID (2001) DOCK 4.0: search strategies for automated molecular docking of flexible molecule databases. J Comput Aided Mol Des 15: 411–428.
12. Goodsell DS, Morris GM, Olson AJ (1996) Automated docking of flexible ligands: applications of AutoDock. J Mol Recognit 9: 1–5.
13. Halgren TA, Murphy RB, Friesner RA, Beard HS, Frye LL, et al. (2004) Glide: a new approach for rapid, accurate docking and scoring. 2. Enrichment factors in database screening. J Med Chem 47: 1750–1759.
14. Friesner RA, Banks JL, Murphy RB, Halgren TA, Klicic JJ, et al. (2004) Glide: a new approach for rapid, accurate docking and scoring. 1. Method and assessment of docking accuracy. J Med Chem 47: 1739–1749.
15. Rarey M, Kramer B, Lengauer T, Klebe G (1996) A fast flexible docking method using an incremental construction algorithm. J Mol Biol 261: 470–489.
16. Bursulaya BD, Totrov M, Abagyan R, Brooks CL (2003) Comparative study of several algorithms for flexible ligand docking. J Comput Aided Mol Des 17: 755–763.
17. Stahl M, Rarey M (2001) Detailed analysis of scoring functions for virtual screening. J Med Chem 44: 1035–1042.
18. Wyss PC, Gerber P, Hartman PG, Hubschwerlen C, Locher H, et al. (2003) Novel dihydrofolate reductase inhibitors. Structure-based versus diversity-based library design and high-throughput synthesis and screening. J Med Chem 46: 2304–2312.
19. Pearlman DA, Charifson PS (2001) Are free energy calculations useful in practice? A comparison with rapid scoring functions for the p38 MAP kinase protein system. J Med Chem 44: 3417–3423.
20. Kollman P (1993) Free-Energy Calculations - Applications to Chemical and Biochemical Phenomena. Chemical Reviews 93: 2395–2417.
21. Aqvist J, Luzhkov VB, Brandsdal BO (2002) Ligand binding affinities from MD simulations. Acc Chem Res 35: 358–365.
22. Kollman PA, Massova I, Reyes C, Kuhn B, Huo SH, et al. (2000) Calculating structures and free energies of complex molecules: Combining molecular mechanics and continuum models. Accounts of Chemical Research 33: 889–897.
23. Huo S, Wang J, Cieplak P, Kollman PA, Kuntz ID (2002) Molecular dynamics and free energy analyses of cathepsin D-inhibitor interactions: insight into structure-based ligand design. J Med Chem 45: 1412–1419.
24. Masukawa KM, Kollman PA, Kuntz ID (2003) Investigation of neuraminidase-substrate recognition using molecular dynamics and free energy calculations. J Med Chem 46: 5628–5637.
25. Kuhn B, Gerber P, Schulz-Gasch T, Stahl M (2005) Validation and use of the MM-PBSA approach for drug discovery. J Med Chem 48: 4040–4048.
26. Ferrara P, Curioni A, Vangrevelinghe E, Meyer T, Mordasini T, et al. (2006) New scoring functions for virtual screening from molecular dynamics simulations with a quantum-refined force-field (QRFF-MD). Application to cyclin-dependent kinase 2. J Chem Inf Model 46: 254–263.
27. Narumi T, Ohno Y, Okimoto N, Koishi T, Suenaga A, et al. (2006) A 185 Tflops simulation of amyloid-forming peptides from Yeast Prion Sup35 with the special-purpose computer System MD-GRAPE3. Proc Supercomputing 2006, in CD-ROM.
28. Taiji M (2004) MDGRAPE-3 chip: a 165 Gflops application specific LSI for molecular dynamics simulations.; 2004. IEEE Computer Society. pp. in CD-ROM.
29. Thomas MP, McInnes C, Fischer PM (2006) Protein structures in virtual screening: A case study with CDK2. J Med Chem 49: 92–104.
30. Kontoyianni M, McClellan LM, Sokol GS (2004) Evaluation of docking performance: comparative data on docking algorithms. J Med Chem 47: 558–565.
31. Wang R, Lu Y, Wang S (2003) Comparative evaluation of 11 scoring functions for molecular docking. J Med Chem 46: 2287–2303.
32. Cho AE, Wendel JA, Vaidehi N, Kekenes-Huskey PM, Floriano WB, et al. (2005) The MPSim-Dock hierarchical docking algorithm: application to the eight trypsin inhibitor cocrystals. J Comput Chem 26: 48–71.
33. Erickson JA, Jalaie M, Robertson DH, Lewis RA, Vieth M (2004) Lessons in molecular recognition: the effects of ligand and protein flexibility on molecular docking accuracy. J Med Chem 47: 45–55.
34. Kua J, Zhang Y, McCammon JA (2002) Studying enzyme binding specificity in acetylcholinesterase using a combined molecular dynamics and multiple docking approach. J Am Chem Soc 124: 8260–8267.
35. Witten IH, Frank E (1999) Data mining: practical machine learning tools and techniques with java implementations. New York: Morgan Kaufmann.
36. Habe H, Morii K, Fushinobu S, Nam JW, Ayabe Y, et al. (2003) Crystal structure of a histidine-tagged serine hydrolase involved in the carbazole degradation (CarC enzyme). Biochem Biophys Res Commun 303: 631–639.
37. Dorfman DD, Berbaum KS, Metz CE (1992) Receiver operating characteristic rating analysis. Generalization to the population of readers and patients with the jackknife method. Invest Radiol 27: 723–731.
38. Hillis SL, Berbaum KS (2005) Monte Carlo validation of the Dorfman-Berbaum-Metz method using normalized pseudovalues and less data-based model simplification. Acad Radiol 12: 1534–1541.
39. Hillis SL, Obuchowski NA, Schartz KM, Berbaum KS (2005) A comparison of the Dorfman-Berbaum-Metz and Obuchowski-Rockette methods for receiver operating characteristic (ROC) data. Stat Med 24: 1579–1607.
40. Roe CA, Metz CE (1997) Variance-component modeling in the analysis of receiver operating characteristic index estimates. Acad Radiol 4: 587–600.
41. Roe CA, Metz CE (1997) Dorfman-Berbaum-Metz method for statistical analysis of multireader, multimodality receiver operating characteristic data: validation with computer simulation. Acad Radiol 4: 298–303.
42. Gohlke H, Case DA (2004) Converging free energy estimates: MM-PB(GB)SA studies on the protein-protein complex Ras-Raf. Journal of Computational Chemistry 25: 238–250.
43. Numata J, Wan M, Knapp EW (2007) Conformational entropy of biomolecules: beyond the quasi-harmonic approximation. Genome Inform 18: 192–205.
44. Chang CE, Chen W, Gilson MK (2005) Evaluating the accuracy of the quasiharmonic approximation. Journal of Chemical Theory and Computation 1: 1017–1028.
45. Davies TG, Bentley J, Arris CE, Boyle FT, Curtin NJ, et al. (2002) Structure-based design of a potent purine-based cyclin-dependent kinase inhibitor. Nat Struct Biol 9: 745–749.
46. Davis ST, Benson BG, Bramson HN, Chapman DE, Dickerson SH, et al. (2001) Prevention of chemotherapy-induced alopecia in rats by CDK inhibitors. Science 291: 134–137.

47. Lamb ML, Jorgensen WL (1997) Computational approaches to molecular recognition. Curr Opin Chem Biol 1: 449–457.
48. Zhou Z, Madura JD (2004) Relative free energy of binding and binding mode calculations of HIV-1 RT inhibitors based on dock-MM-PB/GS. Proteins 57: 493–503.
49. Huang N, Shoichet BK, Irwin JJ (2006) Benchmarking sets for molecular docking. J Med Chem 49: 6789–6801.
50. Kollman PA, Massova I, Reyes C, Kuhn B, Huo S, et al. (2000) Calculating structures and free energies of complex molecules: combining molecular mechanics and continuum models. Acc Chem Res 33: 889–897.
51. Katz BA, Mackman R, Luong C, Radika K, Martelli A, et al. (2000) Structural basis for selectivity of a small molecule, S1-binding, submicromolar inhibitor of urokinase-type plasminogen activator. Chem Biol 7: 299–312.
52. Ala PJ, DeLoskey RJ, Huston EE, Jadhav PK, Lam PY, et al. (1998) Molecular recognition of cyclic urea HIV-1 protease inhibitors. J Biol Chem 273: 12325–12331.
53. Dvir H, Wong DM, Harel M, Barril X, Orozco M, et al. (2002) 3D structure of Torpedo californica acetylcholinesterase complexed with huprine X at 2.1 A resolution: kinetic and molecular dynamic correlates. Biochemistry 41: 2970–2981.
54. MOE. Montreal: Chemical Computing Group Inc.
55. Lipinski CA, Lombardo F, Dominy BW, Feeney PJ (2001) Experimental and computational approaches to estimate solubility and permeability in drug discovery and development settings. Adv Drug Deliv Rev 46: 3–26.
56. Wang R, Fang X, Lu Y, Yang CY, Wang S (2005) The PDBbind database: methodologies and updates. J Med Chem 48: 4111–4119.
57. Wang R, Fang X, Lu Y, Wang S (2004) The PDBbind database: collection of binding affinities for protein-ligand complexes with known three-dimensional structures. J Med Chem 47: 2977–2980.
58. Gray NS, Wodicka L, Thunnissen AMWH, Norman TC, Kwon SJ, et al. (1998) Exploiting chemical libraries, structure, and genomics in the search for kinase inhibitors. Science 281: 533–538.
59. Schrödinger Inc. PortlandOR).
60. Sørenson T (1948) A method of establishing groups of equal amplitude in a plant based on similarity of species content and its applications to analysis of vegetation on Danish commons. Biologiske Skrifter 5: 1–34.
61. Hoffmann D, Kramer B, Washio T, Steinmetzer T, Rarey M, et al. (1999) Two-stage method for protein-ligand docking. J Med Chem 42: 4422–4433.
62. Jorgensen WL, Chandrasekhar J, Madura JD, Impey RW, Klein ML (1983) Comparison of Simple Potential Functions for Simulating Liquid Water. Journal of Chemical Physics 79: 926–935.
63. Case DA, Darden TA, Cheatham TEr, Simmerling CL, Wang J, et al. (2004) AMBER 8 University of California San Francisco.
64. Duan Y, Wu C, Chowdhury S, Lee MC, Xiong G, et al. (2003) A point-charge force field for molecular mechanics simulations of proteins based on condensed-phase quantum mechanical calculations. J Comput Chem 24: 1999–2012.
65. Berendsen HJC, Postma JMP, van Gunsteren WF, DiNola A, Haak JR (1984) Molecular dynamics with coupling to an external bath. J Comput Phys 81: 3684–3690.
66. Wang J, Wolf RM, Caldwell JW, Kollman PA, Case DA (2004) Development and testing of a general amber force field. J Comput Chem 25: 1157–1174.
67. Jakalian A, Jack DB, Bayly CI (2002) Fast, efficient generation of high-quality atomic charges. AM1-BCC model: II. Parameterization and validation. J Comput Chem 23: 1623–1641.
68. Jakalian A, Bush BL, Jack DB, Bayly CI (2000) Fast, efficient generation of high-quality atomic Charges. AM1-BCC model: I. Method. Journal of Computational Chemistry 21: 132–146.
69. Rocchia W, Alexov E, Honig B (2001) Extending the applicability of the nonlinear poisson-boltzmann equation: multiple dielectric constants and multivalent ions. J Phys Chem B 105: 6507–6514.
70. Rocchia W, Sridharan S, Nicholls A, Alexov E, Chiabrera A, et al. (2002) Rapid grid-based construction of the molecular surface and the use of induced surface charge to calculate reaction field energies: applications to the molecular systems and geometric objects. J Comput Chem 23: 128–137.
71. Sitkoff D, Sharp KA, Honig B (1994) Accurate calculation of hydration free energies using macroscopic solvent models. J Phys Chem 98: 1978–1988.
72. Swanson JMJ, Adcock SA, McCammon JA (2005) Optimized radii for Poisson-Boltzmann calculations with the AMBER force field. Journal of Chemical Theory and Computation 1: 484–493.
73. Sanner MF, Olson AJ, Spehner JC (1996) Reduced surface: an efficient way to compute molecular surfaces. Biopolymers 38: 305–320.
74. Levy RM, Karplus M, Kushick J, Perahia D (1984) Evaluation of the Configurational Entropy for Proteins - Application to Molecular-Dynamics Simulations of an Alpha-Helix. Macromolecules 17: 1370–1374.

Chem-Bio Informatics Journal, Vol.10, pp.32-45(2010)

Comparison of binding affinity evaluations for FKBP ligands with state-of-the-art computational methods: FMO, QM/MM, MM-PB/SA and MP-CAFEE approaches

Hirofumi Watanabe[1,2*], Shigenori Tanaka[1,2*], Noriaki Okimoto[3], Aki Hasegawa[3], Makoto Taiji[3*], Yoshiaki Tanida[4], Takashi Mitsui[5], Mariko Katsuyama[5], Hideaki Fujitani[4]

[1]*Graduate School of Engineering, Kobe University, 3-11 Tsurukabuto, Nada, Kobe, Japan*
[2]*JST-CREST*
[3]*RIKEN Advanced Science Institute, Computational Systems Biology Research Group, 61-1 Ono-cho, Tsurumi-ku, Yokohama, Kanagawa 230-0046, Japan*
[4]*Fujitsu Laboratories Ltd., 10-1 Morinosato-Wakamiya, Atsugi 243-0197, Japan*
[5]*Fujitsu Ltd, 9-3, Nakase 1-chome, Mihama-ku, Chiba City Chiba 261-8588, Japan*

**E-mail: watanabe@radix.h.kobe-u.ac.jp, tanaka2@kobe-u.ac.jp, taiji@riken.jp*

(Received October 9, 2009; accepted March 15, 2010; published online April 20, 2010)

Abstract

We compared binding affinity evaluations for 10 FKBP ligands with such state-of-the-art computational methods as FMO, QM/MM, MM-PB/SA, and MP-CAFEE. For the FKBP ligands, we confirmed that each method could provide good correlations between the experimental and computational binding affinities. From the calculated results, we discussed the importance of solvation effect and structural sampling for these methods in detail. In addition, we addressed the issues of computational time and present arguments on the future perspective of the computational binding affinity evaluations.

Key Words: Protein-ligand binding affinity, Fragment molecular orbital method, QM/MM method, MM-PB/SA method, MP-CAFEE method, FKBP

Area of Interest: Molecular Computing

1. Introduction

Recent advances in computational resources and increasing numbers of registered three dimensional (3D) protein structures have accelerated the application of computer simulations to large biomolecular systems. Further, recent progresses of computational methods of evaluation of binding affinity, which are expected to improve drug design efficiency, manifest various features in each method employed [1][2]. For example, the fragment molecular orbital (FMO) method [3] can deal with whole large biomolecules quantum mechanically. In the FMO method, a large molecular system is divided into small fragments, and the conventional molecular orbital (MO) calculations are performed for each fragment and fragment pair. The FMO method overcomes the size limitation of the conventional MO method while maintaining chemical accuracy for energy evaluation. The quantum mechanics/molecular mechanics (QM/MM) method is another method for overcoming the size limitation of quantum chemical methods [4]. In the QM/MM method, a region that requires accurate analysis is studied quantum-mechanically, and other regions are assigned to be studied by classical force field calculations. The molecular mechanics Poisson-Boltzmann surface area (MM-PB/SA) method [5] is often used for binding affinity evaluation as well. In the MM-PB/SA method, the free energy is calculated by using the snapshots of solute molecules obtained from explicit-solvent MD simulation. At this time, the explicit solvent is replaced with implicit models. The massively parallel computation for absolute binding free energy (MP-CAFEE) method [6][7][8][9][10][11] directly evaluates free energy difference by the Bennet acceptance ratio (BAR) method, which can be interpreted as a maximum likelihood estimate of free energy differences [9] from the non-equilibrium work based on the non-equilibrium identity [10][11]. Auxiliary restraints for keeping the ligand position are not employed, while such restraints are used in the standard scheme for evaluation of absolute binding affinities by thermodynamic integration or the free energy perturbation method [1].

Successful results have been published by employing these methods [6][7][8][12][13][14][15][16] which provides us with the expectation that such methods can be put to practical use. In these reports, however, the target proteins were not identical for the different methods. Even if the target proteins were identical, their structures might be different, thus making it difficult to perform reliable comparisons among the different methods. In addition, unsuccessful results of binding affinity evaluations were rarely reported [17]. Thus, it is difficult to determine which methods are useful for each specific situation. To provide the answer for this question, in this paper, we attempt to perform reliable comparisons of binding affinity evaluations among the state-of-the-art calculation methods. To achieve this, we evaluated protein-ligand binding affinity by different methods for the same target protein and ligands, with the same structures. As a test set for binding affinity evaluation, we employed one of the FK506 binding proteins (FKBPs), FKBP12, which is well known as a target protein of the immune suppressor tacrolimus (FK506), and its 10 ligands because this protein is often used as the test set for computational binding affinity evaluations [6][7][14][16].

The computational methods for evaluation of binding affinities are characterized by several aspects such as energy evaluation based on quantum mechanics (QM) or molecular mechanics (MM) force field, a way of incorporating entropic contributions, and solvation effects. To clarify which contributions are important for obtaining good correlations between computational binding affinities and experimental ones, a systematic comparison of results obtained from various computational methods is important. Thus, we used four state-of-the-art computational methods, FMO, QM/MM, MM-PB/SA, and MP-CAFEE, for evaluating the binding affinity of the

protein-ligand bound state. Features of these methods are given in Table 1.

We believe the results of our comparisons will become a benchmark for choosing appropriate methods for practical application. In addition, we expect that they would also become a basis for the development of a new binding affinity evaluation method.

Table 1. Features for each computational method employed in the present study
(* In the MP-CAFEE method, free energy difference is directly evaluated by the BAR method. The entropic contribution is incorporated as a part of free energy difference.)

Method	FMO	QM/MM	MM-PB/SA	MP-CAFEE
Quantum or Classical	Quantum	Quantum + Classical	Classical	Classical
Entropic effect	No	No	Normal mode analysis	BAR method*
Solvation effect	No	No	Implicit (PB equation)	Explicit (TIP3P)
Selection of atomic coordinate	Single Point	Single Point	Sampling by MD	Sampling by MD

2. Methods

2.1 Preparation of protein-ligand structures

The 10 complex structures of FKBP12 and ligands were constructed based on four X-ray crystallographic structures (PDB ID 1FKG (L8), 1FKH (L9), 1FKI (L13) and 1FKF (L20)), where the numbering of the ligand molecules is in accordance with the literature [6][7][18]. As all ligands have common binding elements, a pipecolate and an alpha-keto amide region, we assumed that bound conformations of the other ligands are similar to the known four complexes. Three-dimensional structural image of complex of FKBP and FK-506 (L20) is shown in Figure 1. The molecular formulas of 10 ligands are shown in Figure 2 and the experimental binding affinities and molecular weights are shown in Table 2 [18]. To obtain the initial structures for FMO and QM/MM methods, we performed MM energy minimizations of respective protein-ligand complexes above with the TIP3P water solvent molecules [19] with AMBER 8 [20]. After that, each initial structure of protein-ligand complex for the FMO and QM/MM calculations was constructed by removing water molecules from energy-minimized structure.

2.2 FMO method

For the FMO calculations we used the ABINIT-MP program [21]. The Schrödinger equation was solved by the Hartree-Fock (HF) and Møller-Plesset second order perturbation (MP2) methods with the 6-31G basis set. Fragmentation was performed by the following rule. For the protein region, each fragment has an amino acid residue, and a ligand is included in the fragment. Thresholds for electrostatic interaction approximations [22] such as L_{aoc}, L_{ptc} and L_{dimer} were 0.0, 2.0 and 2.0, respectively. In FMO calculations, we evaluated binding energies without entropies to reduce computational time. We regarded those values as the approximate values of binding free energies.

2.3 QM/MM method

In this article, we used the QSite program for the QM/MM calculations [23]. This software adopts a frozen-core orbital for the QM/MM boundary [4]. The QM region contained side-chain atoms of 7 residues (Tyr26, Asp37, Arg42, Phe46, Trp59, Tyr82, and Phe99), entire atoms of 3 residues (Glu54, Val55, and Ile56) and ligand atoms. The Schrödinger equation for each structure

was solved by the HF and MP2 methods with the 6-31G basis set and the OPLS force field was used for MM region. In the QM/MM calculations, entropic contributions are neglected as well as in the FMO calculations.

2.4 MM-PB/SA method

We performed MD simulations of protein-ligand complexes in explicit water molecules to calculate MM-PB/SA binding free energy. All of the MD simulations were performed using AMBER 8.0 [20] modified for use on the special-purpose computer MDGRAPE-3 [24][25]. All of the protein-ligand complex structures were solvated in a rectangular box containing TIP3P water molecules (explicit solvent) [19] under periodic boundary conditions. The box dimensions were chosen so that the minimum distance of any protein atoms from the wall of the box was 15 Å. The SHAKE algorithm [26] was applied to bonds involving hydrogen atoms, considering an integration time step of 1.0 fs. Long-range Coulomb interactions were treated by applying the particle mesh Ewald (PME) method [27]. The real-space component of the PME method was calculated by using MDGRAPE-3, while the wave number-space component for this method and bonded interactions were calculated by the host computers. To optimize the balance between the calculation times for these components, a cutoff distance of 14 Å was used for the real-space component. Each system was gradually heated to 298 K for the first 50 ps. The Berendsen's temperature and pressure control methods [28] were used to maintain the temperature and pressure constant at 298 K and 1 atm, respectively. The force-field parameters and charges for the protein and ligands which were the same ones as in the MP-CAFEE method, were determined by the force field formulator for organic molecules (FF-FOM) [7]. The production MD trajectory (500 snapshots) was collected for the last period of 5 ns. In the calculation of the binding free energies by the MM-PB/SA method, the water molecules were replaced with implicit solvation models, that is, the PB equation and the SA term, while TIP3P explicit solvent model was employed for obtaining the trajectory. The entropic contribution was evaluated by the normal mode analysis. The evaluations of binding free energy using the MM-PB/SA method have been reported in previous studies [28][29][30][31].

2.5 MP-CAFEE method

The results we show in this paper for the MP-CAFEE method were published by Fujitani et al. [7]. We again show the results by this method in this paper for the comparison with the results by the other methods. Thus, the calculation procedures are to be found in the literature [7]. Here, we summarize the calculation procedure and the setting of the study. We used an in-house modified version of the GROMACS package to perform the MP-CAFEE calculation [32]. MD calculations were performed with the following conditions. A Nose-Hoover thermostat was used for temperature control at 298K and with a time constant of 0.3ps. We used Berendsen's algorithm was employed with time constant of 1.0ps and the pressure of 1.0 atm. In addition, we calculated Coulomb interaction by the PME method. The equilibration process was as follows. First a conjugate gradient minimization was performed, followed by an MD simulation for 200ps with the solute position being restrained. After that, long time equilibration at 298K between the ligand and surrounding system was performed. The equilibration times were 5ns for the solvated ligand and from 10ns to 50ns for solvated protein-ligand complex. After the equilibration, structural samplings for work measurements were performed. In the annihilation process, the Coulomb interaction and van der Waals interaction were turned off by using 32 intermediate λ_i points. For each λ_i point, 12 MD simulations with different initial momenta were performed, where the sampling times for each λ_i point were 2.5 ns for the solvated protein-ligand complex and 1.0 ns for the solvated ligand. The

MD calculations were performed by on a FUJITSU Bioserver test machine with 1920 VLIW architecture processors in a rack. The force fields for both proteins and ligands were determined by the FF-FOM [7], which properly assigns atom types of the general amber force field (GAFF) [33], and RESP charge [34] was used for ligand charges. A more detailed explanation is described in the literature [7].

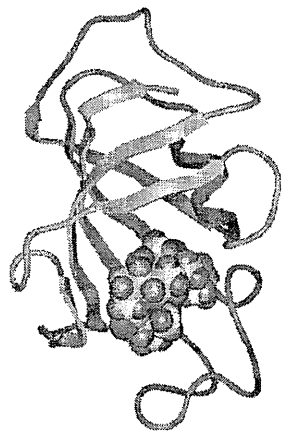

Figure 1. Complex structure of FKBP12, which is composed of 107 residues, and FK506 (L20)

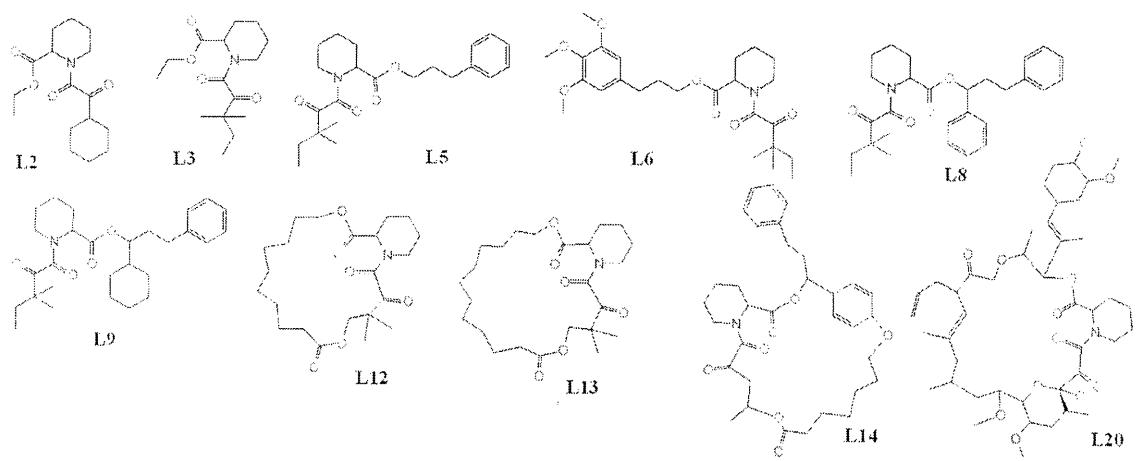

Figure 2. Molecular structures of 10 FKBP ligands, where the numbering of the ligand molecules is in accordance with the literature [6][7][18]

Table 2. Experimental binding free energy of each ligand

ΔG_{exp} and MW indicate the experimental binding affinities and molecular weights for 10 ligands respectively.

Ligand	L2	L3	L5	L6	L8	L9	L12	L13	L14	L20
ΔG_{exp}	-7.8	-8.4	-9.5	-10.8	-10.9	-11.1	-10.3	-9.5	-12.3	-12.8
MW	295.4	283.4	373.5	463.6	449.6	455.6	411.5	437.6	581.4	804.0

3. Results

3.1 FMO method

The correlation between the binding energies evaluated by the FMO method and experimental binding affinities is shown in Figure 3. The results by the FMO-HF and FMO-MP2 [36][37] methods are depicted in Figure 3(a) and (b), respectively, where the 6-31G basis set was used. These figures indicate that the binding energies by the FMO-HF methods were hardly correlated with the experimental values, while the result by the FMO-MP2 method showed better correlation. The bound ligands were surrounded by several hydrophobic residues in the binding pocket. Thus, a better result by the FMO-MP2 method would thus be due to the inclusion of the dispersion force between the ligands and hydrophobic residues. The regression slope was far from unity in the case of the FMO-MP2 (slope=4.13). This result is reasonable, however, because both the entropic contribution and the solvation effect are ignored in the present FMO calculation.

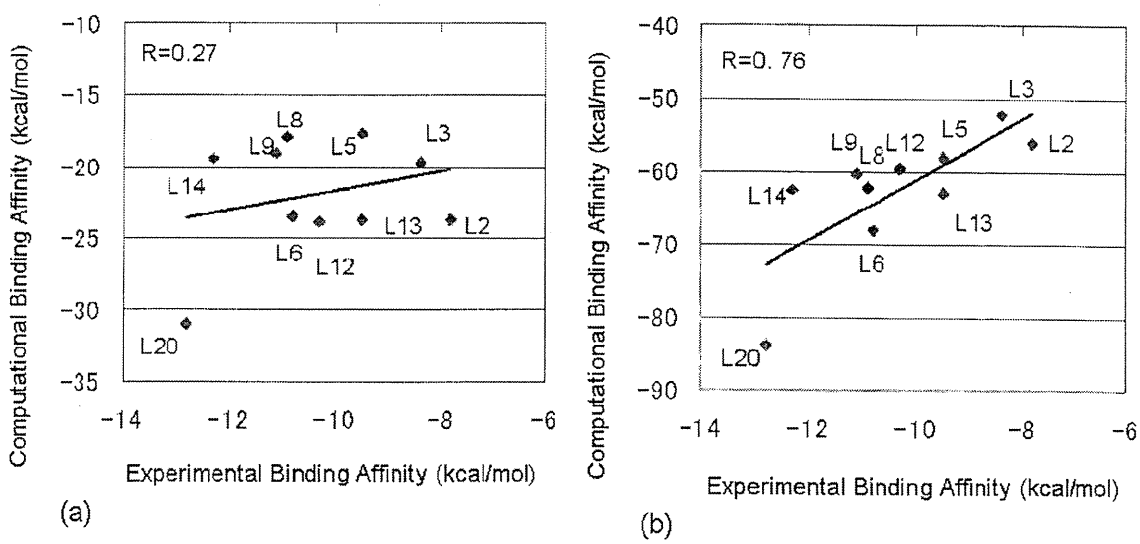

Figure 3. Correlations between the experimental binding affinities and calculated ones by the FMO method, (a) FMO-HF, and (b) FMO-MP2
R is the correlation coefficient.

3.2 QM/MM method

The correlation between binding energies by the QM/MM method and the experimental binding affinities is shown in Figure 4. The QM/MM (HF) and QM/MM (MP2) results are shown in Figure 4(a) and (b), respectively, where the 6-31G basis set was used and the OPLS force field was used for the MM region. The QM/MM (MP2) result (correlation coefficient R=0.86) showed a slightly better correlation than the QM/MM (HF) result (R=0.82). The slopes of regressions, however, were far from unity for both QM/MM (HF) and QM/MM (MP2). In the same way as FMO method, this would be due to the fact the entropic and solvation effects are not included in the present calculations.

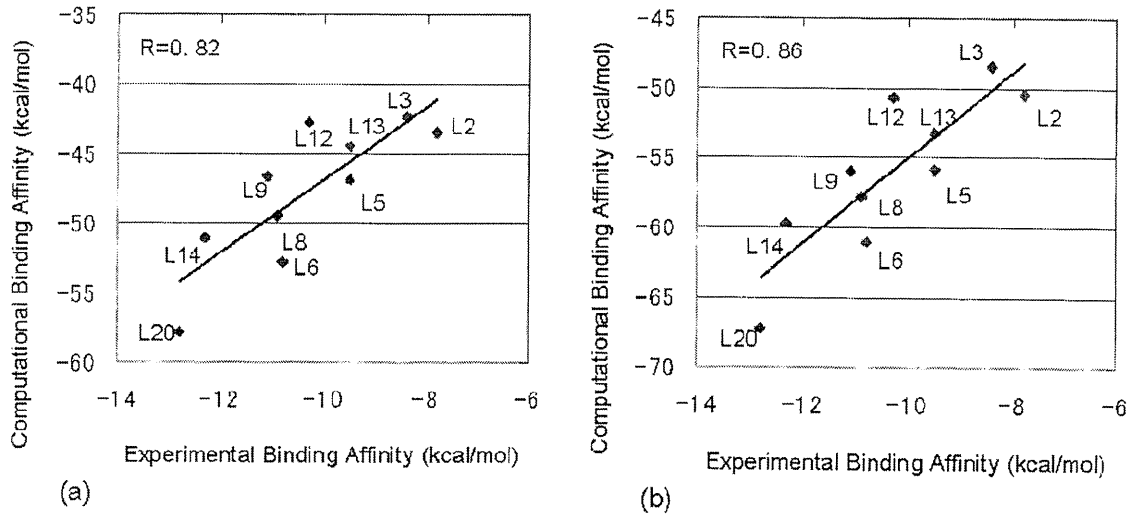

Figure 4. Correlations between the experimental and calculated binding affinities by the QM/MM method, (a) QM/MM HF/6-31G, and (b) QM/MM MP2/6-31G

3.3 MM-PB/SA method

The correlation between binding free energies evaluated by the MM-PB/SA method and experimental binding affinities is shown in Figure 5. In this work, we compared the MM-PB/SA energies with and without entropic term (Figure 5(a) and (b)). This comparison indicated the introduction of the entopic effect improves the absolute binding energies in the MM-PB/SA method, but the MM-PB/SA energies with entropic term show a worse correlation (R=0.76) as compared with the MM-PB/SA energies without entropic term (R=0.83). In addition, for the MM-PB/SA energies with entropic contribution, the slope of regression is far from unity although all the energy components of free energy are incorporated. It is noticeable that these results are in contrast to an earlier binding affinity evaluation for FKBP ligands by the MM-PB/SA method performed by Xu et al. [16]. In their results, the binding affinity evaluation with the entropic contribution provided a better correlation than did the evaluation without the entropic contribution. This difference might be caused by the difference in ligands used for evaluations. In the present evaluation, 4 compounds out of 10 are macrocyclic compounds (see Figure 2). It would be difficult to predict accurate entropic values for these macrocyclic compounds by the normal mode analysis.

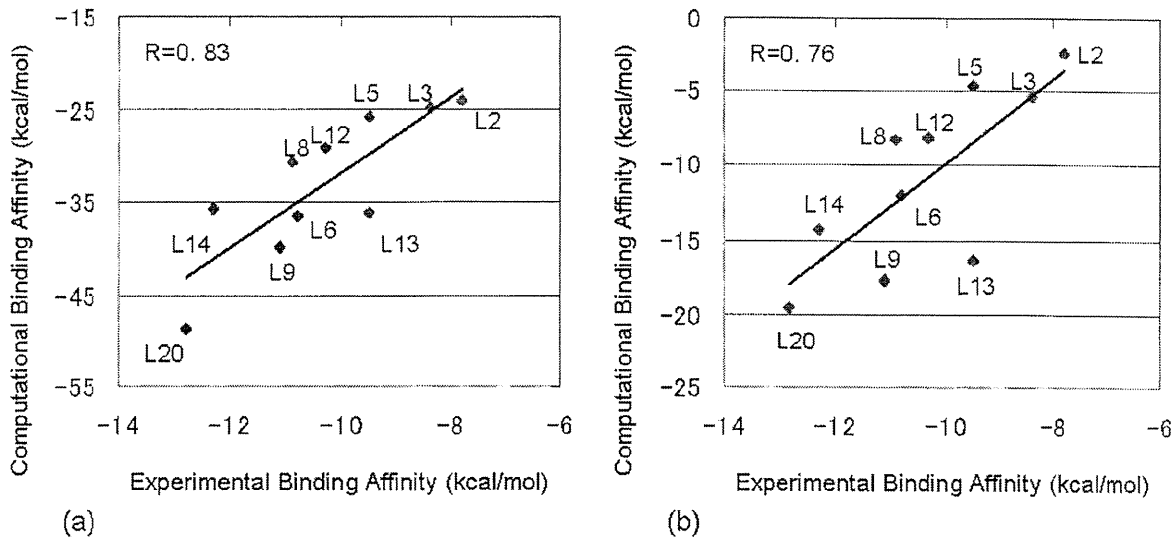

Figure 5. Correlations between the experimental binding affinities and calculated ones by the MM-PB/SA method, (a) without entropy term, and (b) with entropy term

3.4 MP-CAFEE method

The correlation between binding free energies evaluated by the MP-CAFEE method and the experimental binding affinities is shown in Figure 6. This result was previously published in the literature [7] and is shown here for comparison with the other methods. Not only was the correlation very good (R=0.98), but also the slope of regression was 1.26, which is close to unity. In addition, it is remarkable that the calculated absolute binding free energies calculated by this method reproduced the absolute values of the experimental binding affinities.

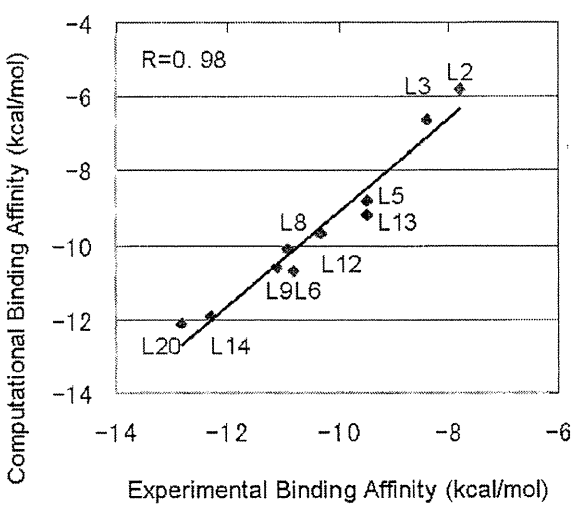

Figure 6. Correlation between the experimental binding affinities and calculated ones by the MP-CAFEE method

4. Discussion

To analyze the relationship between experimental and computational binding affinities, the correlation coefficients, the regressing slopes and intercepts are summarized in Table 3. From this table, it is obvious that MP-CAFEE method showed extremely good correlation with experimental data. The slope of the regression is so close to unity; moreover, the absolute values of the computational binding free energy are so close to those of experimental binding free energies. On the other hand, the other methods show relatively good correlations (correlation coefficients R=0.76-0.86) with experimental results. For the FMO and QM/MM calculations, the correlation coefficients by MP2 level calculations are better than those by the HF calculations. Considering that FKBP ligands interact with the hydrophobic residues in the binding pocket, this improvement is due to the effect of the dispersion force incorporated in the MP2 calculation [38][39]. However, the values of regression slopes deviate from unity since the entropic contribution and the solvation effect are not taken into account in the present FMO and QM/MM calculations. The MM-PB/SA (with entropic term) calculations take into account all contributions approximately, but the slope is far from unity in contrast with that of MP-CAFEE method. To achieve improvement of the correlation coefficient and the regression slope, the precise evaluation of entropic term and incorporation of more accurate solvation energy are essential. In the following, we discuss the importance of solvation effect and structural sampling for these methods in detail.

Table 3. Summary of calculation results

Regression equation is $\Delta G(E)_{comput}$=a ΔG_{exp}+b, where ΔG_{exp}, $\Delta G(E)_{comput}$, a and b are experimental binding affinities, calculated binding free energies (or binding energies), regression slopes and intercepts, respectively. Values in parentheses are standard errors.

Method	FMO (HF)	FMO (MP2)	QM/MM (HF)	QM/MM (MP2)	MM-PB/SA (with entropy)	MM-PB/SA (without entropy)	MP-CAFEE
Correlation	0.27	0.76	0.82	0.86	0.76	0.83	0.98
Intercept: b	-14.98(9.09)	-19.90(13.10)	-20.92(6.69)	-24.28(6.84)	19.13(8.94)	8.67(10.10)	3.56(1.06)
Slope: a	0.69(0.87)	4.13(1.25)	2.60(0.64)	3.07(0.65)	2.90(0.86)	4.04(0.97)	1.26(0.10)

4.1 Structural sampling

Structural sampling is important for two reasons. One is to find the appropriate stable structures, and the other is to cover enough phase space for entropy estimations. Although the structural sampling was not performed into the FMO and QM/MM methods, the fairly good correlations were obtained by these methods. These results may suggest the structural sampling is not important to obtain good correlations for the current target. However, Ishikawa et al. [39] pointed out that appropriate selection of atomic coordinate is crucial to obtain good correlations. Since the structural sampling may contribute to select appropriate atomic coordinates, this would lead to good correlations found in other cases. Further, these methods produce fair correlations in spite of the neglect of entropies. This may be a result of specific structural properties of the current system, or entropy-enthalpy compensation. Since the enthalpy changes are roughly proportional to the entropy changes, the free energy changes, which consist of the sum of both contributions to energy changes, are proportional to enthalpy changes.

In the MM/PB-SA method, the inclusion of the entropic contribution by normal mode analysis made the correlation somewhat worse. In the normal mode analysis, it is known that conformations at different local energy minima provide rather similar entropy values even though there are

differences in the case of finite temperature [40]. One of alternative methods is principal component analysis. The values are sensitive to the data sampling frequency [40][41] and are likely to be overestimated [42]. Therefore, in order to predict more accurate binding free energy by MM/PB-SA method, it is necessary to improve the calculations for the entropy terms. In the MP-CAFFE method, entropic contribution can be treated exactly. If the sampling is enough, the entropy will converge to the theoretical value. The very precise results from the method confirm that the entropic contributions can be estimated precisely after enough structural sampling.

4.2 Solvation effect

Although solvation effect was not incorporated into the FMO and QM/MM methods, relative good correlations were obtained with both of the methods for the current system. Retegan et al. [43] reported that incorporation of solvation effects in semi-empirical QM/MM method significantly improved the correlation between experimental binding affinities and computational binding energies for the CK2 proteins and its ligands. Therefore, introduction of solvation effect into the FMO and QM/MM methods would be one of the improvement means of the correlation coefficients. Furthermore, we discuss the influence of different strategies to treat solvation by MM-based free-energy evaluations. In the MM-PB/SA method, the implicit solvent model described by the PB equation is used for energy evaluation. Many reports suggest that the MM-PB/SA method can provide the fairly good correlation like in the case, and the implicit solvent model seems to be a good and easy way to approximate solvent effects in single-point or short-trajectory calculations [44][45]. In addition, since it was suggested that the implicit solvent model provided slightly worse evaluation of solvation energies than the explicit solvent model did [46], improvement of the implicit solvent model would lead to a better binding affinity evaluation. Also for the solvation energies, the MP-CAFFE method provides the accurate estimations within the framework of classical force fields. It is difficult to distinguish the origin of the difference between the MP-CAFFE and the MM/PB-SA methods, since in the MP-CAFFE method energetic contributions are not estimated separately. As we have already discussed partly, there are several possibilities – solvation effect, entropy estimation, sampling length – and these all will be related to the differences in the results.

4.3 Computational time

Computational time of each method is summarized in Table 4, where the calculation time for the MP-CAFEE method is represented by the converted value in the Pentium4 case for convenience, whereas this calculation was performed with the FUJITSU Bioserver. Although the methods based on the quantum mechanics generally require extensive computational time, the present FMO and QM/MM calculations required less computational time because in the present treatment the structural sampling was not performed in the cases of both QM based methods. If structural sampling were to be performed with the quantum mechanical method, much more computational time would be required. Concerning the classical MD based free energy evaluation method, the MP-CAFEE method required much more computational time than the MM-PB/SA method. This difference is caused by the fact that MP-CAFEE method requires a number of MD runs ($12 \times 32 \times 2$ runs for a FKBP ligand) for obtaining binding affinity of one protein-ligand complex.

Table 4. Typical computational time for the evaluations of binding affinity and of computational resources

Method	FMO (HF)	FMO (MP2)	QM/MM (HF)	QM/MM (MP2)	MM-PB/SA (with entropy)	MM-PB/SA (without entropy)	MP-CAFEE
Typical time	7hours	22hours	2.1hours	1.25days	14days	15days	4.5days
Computational resource	Opteron246 x 16 cores		Xeon5450 3.0GHZ		Xeon5150+MD-GRAPE3		Pentium4 x 300cores

4.4 Further Perspectives

We will discuss the future perspective of computational binding affinity evaluation for drug designs. Although the four state-of-the-art methods discussed here require large computational resources, such computation will become daily in near future by continuous growth of computer performance. We believe our present analysis would provide an important basis for making practical use of the computational binding affinity evaluation. To provide the significant information for practical use, we should continue to work on the comparison of binding affinity evaluation. Current results with only one target protein are not enough to clarify merits and demerits of each method in different situations. This paper is just the first report of our attempt. When many target proteins will have been studied for the comparison of the state-of-the-art methods, our aim will truly be achieved. We will report our next comparison results based on other target proteins.

In this paper we have mainly discussed the correlation coefficients between experimental and computational binding affinities. Although this focused point is suitable for judging which effect is important for reproducing experimental binding affinity, other points would also be needed to satisfy the aim of practical use in drug design because there are many kinds of demands in the pharmaceutical industry. For example, throughput of the screening should be at least more than 100 compounds per week for practical use. Prediction in weak affinity region is important for the fragment-based drug design, since the affinity of a small fragment, which will form the skeleton of lead compound, is very weak. To answer these kinds of questions, the way to assess the computational methods should be reconsidered.

5. Conclusion

To clarify the merits and demerits of various computational approaches for binding free-energy estimation in drug design, we compared the results of the binding energy evaluations by the four state-of-the-art computational methods, such as the FMO, QM/MM, MM-PB/SA and MP-CAFEE methods. We assessed the computational binding affinity evaluation methods from several aspects such as correlation with experimental binding affinity, slope of the regression and computational costs, and discussed which contributions are related to the good correlation.

Acknowledgments

The authors are highly grateful to the CBI society for the accomplishment of this work. A plan of this study was born at the site of the CBI annual meeting in 2007. In the symposium on the last day of this meeting, successful results of the FMO, MM-PB/SA and MP-CAFEE methods were reported. At that time, to clarify more detailed applicability of each method, this comparative study was proposed. In addition, this work is based on presentations in a workshop "Present Status and

Problems of *in silico* Technology in Structure Based Drug Design", which was held as a parallel session of the annual meeting of the CBI society in 2008. The authors also acknowledge all the participants of this workshop. We thank Drs. Yoshio Okiyama and Ikuo Kurisaki for useful comments on the manuscript. This work was partially supported by the CREST project of the Japan Science and Technology Agency (JST).

References

[1] M. K. Gilson, J. A. Given, B. Bush, and J. A. McCammon, The statistical-thermodynamic basis for computation of binding affinities, A critical review, *Biophys. J.*, **72**.1047-1069 (1997).

[2] M. K. Gilson and H. Zhou, Calculation of Protein-Ligand Binding Affinities, *Annu. Rev. Biophys. Biomol. Struct.*, **36**, 21-42 (2007).

[3] K. Kitaura K, E. Ikeo E, T. Asada, T. Nakano and M. Uebayasi, Fragment molecular orbital method: an approximate computational method for large molecule, *Chem. Phys. Lett.*, **313**, 701-706 (1999).

[4] D. M. Philipp and R. A. Friesner, Mixed ab initio QM/MM modeling using frozen orbitals and tests with alanine dipeptide and tetrapeptide, *J. Comput. Chem.*, **20**, 1468-1494 (1999).

[5] J. Srinivasan, J. Miller J, P. A. Kollman, D. A. Case, Continuum solvent studies of the stability of RNA hairpin loops and helices, *J. Biomol. Struct. Dyn.*, **16**, 671-682 (1998).

[6] H. Fujitani, Y. Tanida, M. Ito, G. Jayachandran, C. D. Snow, M. R. Shirts, E. J. Sorin and V. S. Pande, Direct calculation of the binding energies of FKBP ligands, *J. Chem. Phys.*, **123**, 084108 (2005).

[7] H. Fujitani, Y. Tanida and A. Matsuura, Massively parallel computation of absolute binding free energy with well-equilibrated states, *Phys. Rev. E*, **79**, 021914 (2009).

[8] Y. Tanida, M. Ito and H. Fujitani., Calculation of absolute free energy of binding for theophylline and its analog to aptamer using nonequilibrium work values, *Chem. Phys.*, **337**, 135-143 (2007).

[9] M. R. Shirts, E. Bair, G. Hooker and V. S. Pande, Equilibrium free energies from nonequilibrium measurements using maximum likelihood methods, *Phys. Rev. Lett.*, **91** 140630 (2003).

[10] C. Jarzynski, Nonequilibrium Equality for Free Energy Differences, *Phys. Rev. Lett.*, **78**, 2690 (1997).

[11] G. E. Crooks, Path-ensemble averages in systems driven far from equilibrium, *Phys. Rev. E*, 61, 2361 (2000).

[12] K. Fukuzawa, K. Kitaura, K. Uebayasi, K. Nakata, T. Kaminuma and T. Nakano, Ab initio quantum mechanical study of the binding energies of human estrogen receptor α with its ligands: an application of fragment molecular orbital method, *J. Comput. Chem.*, **26**, 1-10 (2005).

[13] T. Harada, K. Yamagishi, T. Nakano, K. Kitaura and H. Tokiwa, Ab initio fragment molecular orbital theory of ligand binding to human progesterone receptor ligand binding domain, *Naunyn-Schmiedeberg's Arch Pharmacol*, **377**, 607-615 (2008).

[14] I. Nakanishi, D. G. Fedorov and K. Kitaura, Molecular Recognition Mechanism of FK506 Binding Protein: An All-Electron Fragment Molecular Orbital Study, *Proteins*, **68**, 145-158 (2007).

[15] P. A. Kollman, I. Massova, C. Reyes, B. Kuhn, S. Huo, L. Chong, M. Lee, T. Lee, Y. Duan, W. Wan, O. Donini, P. Cieplak, J. Srivivasan, D. A. Case and T. E. Cheatham III,

Calculating structures and free energies of complex molecules: combining molecular mechanics and continuum models, *Acc. Chem. Rev.*, **33**, 889-897 (2000).

[16] Y. Xu and R. Wang, A Computational of Analysis of the Binding Affinities of FKBP12 Inhibitors Using the MM-PB/SA Method, *Proteins*, **64**, 1058-1068 (2006).

[17] D. A. Pearlman, Evaluating the molecular mechanics Poisson-Boltzmann surface area free energy method using a congeneric series of ligands to p38 MAP kinase, *J. Med. Chem.*, **48**, 7796-7807 (2005).

[18] D. A. Holt, J. I. Luengo, D. S. Yamashita, H. J. Oh, A. L. Konialian, H. K. Yen, L. W. Rozamus, M. Brandt, M. J. Bossard, M. A. Levy, D. S. Eggleston, J. Liang, L. W. Schultz, T. J. Stout and J. Clardy, Design, synthesis, and kinetic evaluation of high-affinity FKBP ligands and the X-ray crystal structures of their complexes with FKBP12, *J. Am. Chem. Soc.*, **115**, 9925-9938 (1993).

[19] W. L. Jorgensen, J. Chandrasekhar, J. D. Madura, R. W. Impey and M. L. Klein, Comparison of Simple Potential Functions for Simulating Liquid Water, *J. Chem. Phys.*, **79**. 926-935 (1983).

[20] D. A. Case, T. A. Darden, T. E. Cheatham, III, C. L. Simmerling, J. Wang, R. E. Duke, R. Luo, K. M. Merz, B. Wang, D. A. Pearlman, M. Crowley, S. Brozell, V. Tsui, H. Gohlke, J. Mongan, V. Hornak, G. Cui, P. Beroza, C. Schafmeister, J. W. Caldwell, W. S. Ross, and P. A. Kollman. AMBER 8, *University of California San Francisco* (2004).

[21] T. Nakano, T. Kaminuma, T. Sato, Y. Akiyama, M. Uebayasi and K. Kitaura, Fragment molecular orbital method: application to polypeptides, *Chem. Phys. Lett.*, **318**, 614-618 (2000).

[22] T. Nakano, T. Kaminuma, T. Sato, K. Fukuzawa, Y. Akiyama, M. Uebayasi and K. Kitaura, Fragment molecular orbital method: use of approximate electrostatic potential, *Chem. Phys. Lett.*, **351**, 475-480 (2002).

[23] Schrödinger Inc. Portland, OR. http://www.schrodinger.com/

[24] M. Taiji, MDGRAPE-3 chip: a 165 Gflops application specific LSI for molecular dynamics simulations, *Proceedings of Hot Chips 16, IEEE Computer Society, in CD-ROM.* (2004).

[25] T. Narumi, Y. Ohno, N. Okimoto, T. Koishi, A. Suenaga, N. Futatsugi, R. Yanai., R. Himeno, S. Fujikawa, M. Ikei and M. Taiji . A 185 Tflops simulation of amyloid-forming peptides from Yeast Prion Sup35 with the special-purpose computer System MD-GRAPE3, *Proc Supercomputing 2006, in CD-ROM* (2006).

[26] J. P. Ryckaert, G. Ciccotti and H. J. C. Berendsen, Numerical-Integration of Cartesian Equations of Motion of a System with Constraints - Molecular-Dynamics of N-Alkanes, *J. Comput. Phys.*, **23**, 327-341 (1977).

[27] T. Darden, D. York and L. Pedersen, Particle Mesh Ewald - an N.Log(N) Method for Ewald Sums in Large Systems, *J. Chem. Phys.*, **98**, 10089-10092 (1993).

[28] H. J. C. Berendsen and J. P. M. Postma, W. F. Vangunsteren, A. Dinola, J. R. Haak, Molecular-Dynamics with Coupling to an External Bath, *J. Chem. Phys.*, **81**. 3684-3690 (1984).

[29] A. Suenaga, M. Hatakeyama, M. Ichikawa, X. Yu, N. Futatsugi, T. Narumi, K. Fukui, T. Terada and M. Taiji, M. Shirouzu, S. Yokoyama, A. Konagaya, Molecular dynamics, free energy, and SPR analyses of the interactions between the SH2 domain of Grb2 and ErbB phosphotyrosyl peptides, *Biochemistry*, **42**, 5195-5200 (2003).

[30] A. Suenaga, N. Takada, M. Hatakeyama, M. Ichikawa, X. Yu, K. Tomii, N. Okimoto, N. Futatsugi, T. Narumi, M. Shirouzu, S. Yokoyama, A. Konagaya and M. Taiji, Novel mechanism of interaction of p85 subunit of phosphatidylinositol 3-kinase and ErbB3 receptor-derived phosphotyrosyl peptides, *J. Biol. Chem.*, **280**, 1321-1326 (2005).

[31] N. Okimoto, T. Nakamura, A. Suenaga, N. Futatsugi, Y. Hirano, Y. Yamaguchi and T. Ebisuzaki, Cooperative motions of protein and hydration water molecules: Molecular dynamics study of scytalone dehydratase, *J. Am. Chem. Soc.*, **126**, 13132-13139 (2004).
[32] http://www.gromacs.org/
[33] J. Wang, R. M. Wolf, Caldwell, J. W.;P. A. Kollman and D. A. Case, Development and testing of a general AMBER force field, *J. Comput. Chem.*, 25, 2004, 1157-1174.
[34] C. I. Bayly, P. Chieplak, W. D. Cornell and P. A. Kollman, A Well Behaved Electrostatic Potential Based Method Using Charge Restraint deriving Atomic Charges: The RESP model, *J. Phys. Chem.*, **97**, 10268-10280 (1993).
[35] Y. Mochizuki, S. Koikegami, T. Nakano, S. Amari, and K. Kitaura, Large scale MP2 calculations with fragment molecular orbital scheme, *Chem. Phys. Lett.*, **396,** 473-479 (2004).
[36] Y. Mochizuki, T. Nakano, S. Koikegami, S. Tanimori, Y. Abe, U. Nagashima, and K. Kitaura, A parallelized integral-direct second-order Moeller-Plesset perturbation theory method with a fragment molecular orbital scheme, *Theor. Chem. Acc.*, **112**, 442-452 (2004).
[37] K. Fukuzawa, Y. Mochizuki, S. Tanaka, K. Kitaura, and T. Nakano, Molecular Interactions between Estrogen Receptor and Its Ligand Studied by the Ab Initio Fragment Molecular Orbital Method, *J. Phys. Chem. B,* **110**, 16102-16110 (2006).
[38] K. Fukuzawa, Y. Komeiji, Y. Mochizuki, A. Kato, T. Nakano and S. Tanaka, Intra- and Inter-molecular Interactions between Cyclic-AMP Receptor Protein and DNA: Ab initio Fragment Molecular Orbital Study, *J. Comput. Chem.*, **27**, 948-960 (2006).
[39] T. Ishikawa, T. Ishikura and K. Kuwata, Theoretical study of the prion protein based on the fragment molecular orbital method, *J. Comput. Chem.*, **30**, 2594-2601, (2009).
[40] H. Gohlke and D. A. Case, Converging free energy estimates: MM-PB(GB)SA studies on the protein-protein complex Ras-Raf, *J. Comput. Chem.*, **25**, 238-250 (2004).
[41] J. Numata, M. Wan and E. W. Knapp, Conformational entropy of biomolecules:beyond the quasi-harmonic approximation, *Genome Inform.*, **18**, 192-205 (2007).
[42] C. E. Chang, W. Chen and M. K. Gilson, Evaluating the accuracy of the quasiharmonic approximation, *J. Chem. Theor. Comput,* **1**, 1017-1028 (2005).
[43] M. Retegan, A. Milet and H. Jamet, Exploring the Binding of Inhibitors Derived from Tetrabromobenzimidazole to the CK2 Protein Using a QM/MM-PB/SA Approach, *J. Chem. Inf. Model*, **49**, 963-871 (2009).
[44] B. Kuhn, P. Gerber, T. Schulz-Gasch and M. Stahl, Validation and use of the MM-PBSA approach for drug discovery, *J. Med. Chem.*, **48**, 4040-4048 (2005).
[45] S. Huo, J. Wang, P. Cieplak, P. A. Kollman and I. D. Kuntz, Molecular dynamics and free energy analyses of cathepsin D-inhibitor interactions: insight into structure-based ligand design, *J. Med. Chem.*, **45**, 1412-1419 (2002).
[46] A. Nicholls, D. L. Mobley, J. P. Guthrie, J. D. Chodera, D. I. Bayly, M. D. Cooper and V. J Pande, Predicting small-molecule solvation free energies: an informal blind test for computational chemistry, *J. Med. Chem.*, **51**, 769-779 (2008).

高性能計算による薬剤分子設計

[1]理化学研究所　生命システム研究センター　生命モデリングコア計算分子設計研究グループ

[2]計算科学研究機構　プロセッサ研究チーム

泰地　真弘人[12]、沖本　憲明[1]

taiji@riken.jp, okimoto@gsc.riken.jp

高性能計算機の発展と計算科学

電子計算機は、1946 年に ENIAC が完成して以来ほぼ 5 年で 10 倍のペースで発展を続けており、2011 年には 10PFLOPS(10^{16} 演算/秒)の性能に到達する見込みである。さらに今後も、10 年ぐらいは同等のペースでの発展が期待される。その性能向上は主に半導体技術の発展に支えられてきた。しかし、単体プロセッサの動作速度は電力や配線遅延などの制約により限界に到達してしまい、それでも集積度の向上は継続しているため、近年では高並列処理技術なしでは性能向上が見込めなくなっている。今後は、100 万以上の大規模な並列化に取り組む必要があり、ハードウェア開発のみならずソフトウェア開発の超大規模並列化が重要な研究開発課題となっている。計算科学においても、並列化を重視した計算アルゴリズム・ソフトウェア開発が必須になりつつある。また、分子設計などでは探索のために多量の計算を行う必要がある。計算資源の増大につれ、1 万以上のシミュレーションを実行しデータ処理を行うようなことが日常的に行われるようになると、計算やエラー処理の自動化、計算結果や初期値のデータベース化などが重要になる。こうした計算の周辺技術の取り込みも今後の重要な課題である。いずれにせよ、1PFLOPS-1EFLOPS という巨大な計算資源をいかにうまく使い、科学的成果・技術的創出を達成できるかが計算科学に今後問われている課題である。次に説明する京コンピュータの利用をきっかけに、大規模計算資源を実際の成果に結びつけていくための開発が一層進むことが期待される。

京コンピュータ

京コンピュータは、現在理化学研究所と富士通株式会社で開発を進めているスーパーコンピュータである（図 1)。LINPACK ベンチマークで 10PFLOPS の性能を出すことも一つの性能目標であるが、科学的成果の創出に向けてアプリケーションの実効性能が重視されている。実際、他の世界トップクラスの計算機と比較すると、高性能計算に向けた最適化が随所に見られる。システムの完成は 2012 年度を予定しており、その年の秋から本格的な供用が開始される計画である。開発は順調に推移しており、部分的に稼働させたシステムを用いた LINPACK ベンチマークで既に 8.16PFLOPS の性能を達成し、2011 年 6 月の TOP500 リスト[1]で 1 位を飾った。その時の実行効率は 93%に達し、大規模システムでありながら高い効率を達成している。また、電力効率を競う Green 500[2]においても同時に 6 位の性能を達成した。電力効率 1, 2 位の汎用機 BlueGene/Q は別格であるが、京コンピュータはその他 GPU を用いたシステム群とほぼ互角である。GPU では実アプリケーションの実行効率は京コンピュータより低いものが多いと考えられるので、実質的には BlueGene/Q に次いで 2 位の性能であると考えられる。これらの優れた実行効率・電力効率は高いメモリ・ネットワーク帯域、水冷の採用など高性能計算(High Performance Computing, HPC)専用設計の賜物である。今後の大規模システムでは電力性能が大きな制約になることが明らかであり、京コンピュータはその面でも重要な一歩である。

京コンピュータは 8 万個以上のプロセッサを並列

につないだ大規模並列システムシステムである。さらに、1 個のプロセッサは 8 個のコアを持つので、コアの数としては 64 万以上となる。さらに、1 個のコアは 4 個の積和演算器を持つので、積和演算器の数としては 256 万個以上となり、その効率的な利用には非常に大きな並列度が必要である。

京コンピュータを特徴づける技術は、①HPC 向けの機能を持つプロセッサ“SPARC64 VIIIfx[3]”②高速で HPC 向けの機能を持つ 6 次元 Mesh-Torus ネットワーク“Tofu[4]”である。これらにより、柔軟で有効性の高い並列実行を可能としている。例えば、分子動力学計算のカーネルの実行では、50%以上の実行効率が得られている[5]。

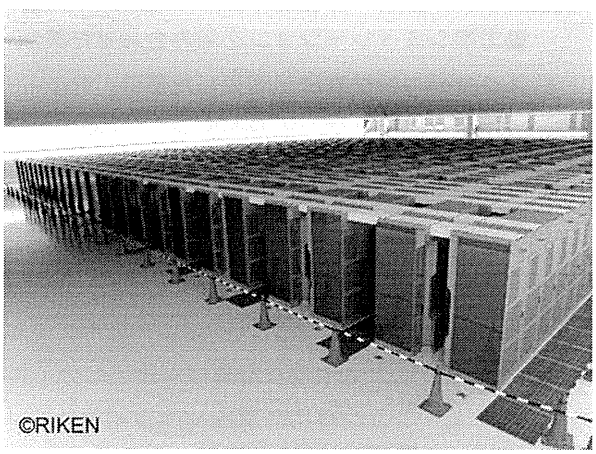

図 1. 京コンピュータの写真。（理研次世代スーパーコンピュータ開発実施本部提供）

分子シミュレーションによる薬剤スクリーニング

我々のグループの目標は、京コンピュータなどのスーパーコンピュータを活用した、大規模計算による分子設計の実現である。長期的には、酵素の設計や、複数のタンパク質が組み合わさってできる構造などの大きな機能分子の設計を目指しているが、現在はまず低分子やペプチド設計など比較的小さな分子をターゲットにした計算手法の検討を進めている。ここでは、ドッキング計算と分子シミュレーションを結合した高精度なスクリーニング手法の研究について紹介する。

タンパク質等の生体高分子と低分子の結合親和性は、阻害剤の設計において最も重要なパラメータの一つであり、これまで多くの計算手法の開発が行われてきた。特に近年では、多くのタンパク質・タンパク質−基質複合体の立体構造が実験的に求められ、Protein Data Bank[6]を初めとする公共データベースに蓄積されてきた。その結果、タンパク質の構造をベースにした薬剤設計“Structure-Based Drug Design(SBDD)”手法が盛んになった。SBDD にも、実験を中心した方法・計算を中心にした方法と様々であるが、タンパク質の構造が決まればあとは計算で合理的な設計ができれば理想的である。そのため計算による SBDD 手法の開発が古くから進められてきた。

その中でも分子ドッキングは、現在最も標準的に用いられている手法である[7][8][9]。一般的な分子ドッキング手法では、タンパク質を剛体として扱い、そのポケット部位に低分子をフレキシブルに当てはめ、親和性をスコア関数に基づき評価する。しかし、実際のタンパク質の構造は生体環境下で揺らいでおり、また基質結合に伴い大きな構造変化を起こす場合もある。従って、タンパク質によっては、分子ドッキングによるスクリーニングが十分に機能しないことも少なくない。これに対し分子動力学(MD)シミュレーションにより、タンパク質−基質の系全体に対しシミュレーションを行えば、こうしたタンパク質の柔軟性や溶媒の効果を陽に取り込むことができる。但し、MD シミュレーションはドッキングに対し遙かに計算量が多い。それ故、分子設計などの大量計算が必要なものに対する MD シミュレーションの適用は限定的であった。しかし京コンピュータなどの大規模な計算資源の登場により、シミュレーションに基づく分子設計が現実的な手法となりつつある。

我々のグループでは、分子ドッキングに基づく結合構造探索と分子シミュレーションに基づく結合自由エネルギー評価を組み合わせた手法開発を進めている[10]。分子ドッキング手法では、遺伝的アルゴリズムなどの手法を用いて低分子の配位空間を高速に探索することができる。実際に、実験的に得られている複合体構造を高い精度で予測することが可能になっている。しかし前述のように、異なる低分子間での結合親和性の強さを比較するには、分子ドッキングのスコア関数は不安定である。

一方、分子シミュレーションで低分子をタンパク質に結合させる過程を一からシミュレーションすると、シミュレーション時間がマイクローミリ秒オーダーになってしまうと考えられ、現実的でない。また実験的な結合構造は限られた基質−タンパク質にしかないので利用不可能である。そこで、分子ドッキングによって得られた複数の結合構造を基に分子シミュレーションを行い、結合親和性を評価する手法を開発した。

この手法の概念図を図2に示す。まず化合物ライブラリからケモインフォマティクス・Ligand-Based Drug Designの手法を用いて、数万−数十万程度の候補化合物を選ぶ。その後分子ドッキングを用いて、数百ー数千程度まで候補を絞り込むと同時に、複合体構造の候補を得る。この候補構造を出発点に分子動力学シミュレーションを行い、結合自由エネルギーを評価する。分子動力学シミュレーションによる結合自由エネルギー評価にはいくつかの手法があるが、ここでは比較的計算量の少ないMM/PB-SA(Molecular Mechanics/Poisson-Boltzmann

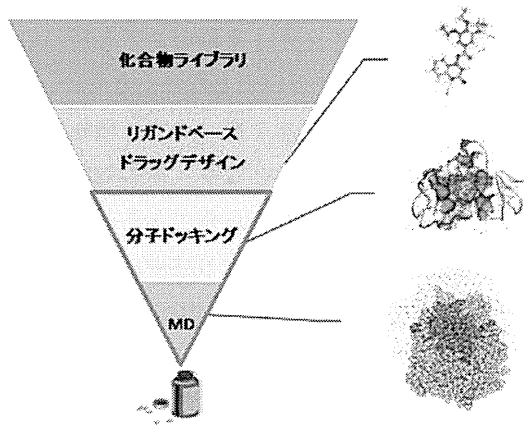

図2. 段階的なスクリーニングにより数百万の化合物ライブラリから数十ー数百の候補化合物を絞り込む過程。最後の分子ドッキングと分子動力学シミュレーションを組み合わせた薬剤スクリーニング手法が開発した部分。分子ドッキングにより結合構造を生成し、それに対し分子シミュレーションで結合親和性を高精度に求める。

SurfaceArea)法[11]で評価を行っている。ここでは、各複合体構造に対し約1ナノ秒のシミュレーションを行った。こうした大規模な計算は、後述の分子動力学シミュレーション専用計算機MDGRAPE-3の利用により可能になった。

数種類のタンパク質(Trypsin, HIV-1 protease, Acetylcholine esterase)に対しこの手法を適用した結果を図3に示す。図は濃縮率を示しており、曲線が左上に行くほど性能が高い。分子シミュレーションの適用により、より高精度な評価が安定して行えることがわかった。